ISSN 1070-3284, Russian Journal of Coordination Chemistry, 2021, Vol. 47, No. 1, pp. 1–9. © Pleiades Publishing, Ltd., 2021.
Russian Text © The Author(s), 2021, published in Koordinatsionnaya Khimiya, 2021, Vol. 47, No. 1, pp. 3–12.

Iron(III) Complexes Based on *N*-Benzylidene-2-Hydroxy-3,5-Di-*tert*-Butylaniline

I. V. Ershova[a], A. S. Bogomyakov[b], S. P. Kubrin[c], A. V. Cherkasov[a], and A. V. Piskunov[a, *]

[a] *Razuvaev Institute of Organometallic Chemistry, Russian Academy of Sciences, Nizhny Novgorod, Russia*
[b] *International Tomography Center, Siberian Branch, Russian Academy of Sciences, Novosibirsk, Russia*
[c] *Research Institute of Physics, Southern Federal University, Rostov-on-Don, Russia*
**e-mail: pial@iomc.ras.ru*

Received April 18, 2020; revised May 28, 2020; accepted June 5, 2020

Abstract—Five-coordinate iron(III) complexes, $(ImPh)_2FeX$ (X = Cl (**I**), Br (**II**), I (**III**), N_3 (**IV**)) containing two bidentate Schiff bases (*N*-benzylidene-2-hydroxy-3,5-di-*tert*-butylaniline (ImPh)H) and a halogen atom/azide group in the coordination sphere were synthesized and characterized in detail. According to the magnetic susceptibility measurements for polycrystalline samples of **I**–**IV** and Mössbauer spectroscopy data in the 2–300 K range, the complexes contain a high-spin metal ion (HS Fe^{3+}, d^5, $S_{Fe} = 5/2$). Compounds **I**–**IV** are stable in the crystalline state in the absence of oxygen or air moisture; however, in solution, they undergo symmetrization, resulting in the formation of the tris-ligand complex $(ImPh)_3Fe$ (**V**), which was also synthesized by the reaction (ImPh)H and $FeCl_3$ (3 : 1). Unlike five-coordinate complexes **I**–**IV**, six-coordinate complex **V** contains low-spin iron(III) ion (LS Fe^{3+}, d^5, $S_{Fe} = 1/2$). The molecular structure of **I** was determined by X-ray diffraction (CIF file CCDC no. 1996527).

Keywords: iron(III), Schiff bases, spin state, magnetic properties, X-ray diffraction, Mössbauer spectroscopy
DOI: 10.1134/S1070328421010012

INTRODUCTION

Iron(III) coordination compounds are of great interest for researchers all over the world, since, along with iron(II) complexes, they are the most common class of compounds that demonstrate the spin-crossover (SCO) phenomenon [1–3]. Spin crossover means switching of the spin state of the complex upon temperature or pressure change [4] or, more rarely, under the action of light [5–7] or magnetic field [8]. Switching between the high-spin (HS) and low-spin (LS) states of the complex is accompanied by a change in its physical properties (magnetic moment, color, dielectric constant, and electrical resistance); therefore, SCO-active compounds are highly promising candidates for the use as molecular magnets, sensors, and components of multifunctional materials [9]. The active search for SCO systems is carried out not only experimentally, but also by theoretical methods [10–15]. Unlike iron(II) complexes, iron(III) compounds are, most often, resistant to oxidation in air, which makes them more promising for potential use in future devices. Currently, derivatives containing multidentate Schiff bases (symmetric and asymmetric ligands based on salicylaldehyde or acetylacetone) are the most numerous and well-studied SCO-active Fe(III) complexes [2, 3]. However, irrespective of the denticity of the ligands (tri- (N_2O, SNO), tetra- (N_2O_2), penta- (N_3O_2), or hexadentate (N_6, N_4O_2) Schiff bases), the Fe^{3+} coordination sphere is filled in such a way that the central ion occurs in an octahedral coordination environment, in which the spin transition occurs between HS (S_{Fe}= 5/2) and LS (S_{Fe} = 1/2) states. An exception is provided by the five-coordinate iron(III) nitrosyl derivatives (FeN_3O_2 core) containing a tetradentate N_2O_2 ligand and an NO molecule in the coordination sphere [16–22]. These compounds tend to undergo a spin transition between the low- and intermediate-spin (IS) states: LS (S_{Fe} = 1/2) ↔ IS (S_{Fe} = 3/2). Five-coordinate iron(III) porphyrin compounds are characterized by a labile spin state of the metal ion (HS–IS) [23]; the HS (S_{Fe} = 5/2) ↔ IS (S_{Fe} = 3/2) spin transition, rare for such spin systems, was detected for the $[Fe^{III}(OMTArP)(H_2O)]ClO_4$ complex where OMTArP is the peripherally substituted octamethyltetraphenylporphyrin [24]. Another class of SCO-active five-coordinate iron(III) complexes are bis-*o*-iminobenzosemiquinone derivatives, $(ImSQ^R)_2Fe^{III}X$ (ImSQ is singly reduced R-phenyl-substituted *o*-iminobenzoquinone, X is inorganic anion) [25–29]. Fine-tuning of the spin state of the Fe^{3+} ion (HS (S_{Fe} = 5/2) or IS (S_{Fe} = 3/2)) by both varying the substituent X (X = Hal, N_3, NCO, NCS) and introducing substituents R (H, Me, OMe) into the

redox active ImSQ ligand enables the HS ($S_{Fe} = 5/2$) ↔ IS ($S_{Fe} = 3/2$) spin transition in $(ImSQ^R)_2Fe^{III}X$. According to a recent theoretical study of a series of tetragonal-pyramidal complexes $(ImSQ^H)_2FeX$ (X = halide/pseudohalide), the observed spin transition is caused by combination of properties of O,N-chelating ImSQ ligands and the apical ligand X [30].

The goal of the present study is to experimentally confirm the key role of radical anion ImSQ ligands for implementation of the spin-crossover in five-coordinate derivatives with the FeN_2O_2X coordination core. We synthesized a series of five-coordinate iron(III) derivatives $(ImPh)_2FeX$ (X = Hal, N_3) using the diamagnetic analogue of the ImSQ ligand *N*-benzylidene-2-hydroxy-3,5-di-*tert*-butylaniline (ImPh)H.

EXPERIMENTAL

All operations on the synthesis of iron complexes were carried out in the absence of atmospheric oxygen and moisture. The solvents used in the study were purified as recommended [31]. The following commercial chemicals (Aldrich) were used: iron(III) chloride, potassium bromide, potassium iodide, sodium azide, and triethylamine. The (ImPh)H ligand was synthesized by a reported procedure [32]. Elemental analysis was carried out on an Elementar Vario EL cube elemental analyzer. Mass spectra were recorded on a Polaris Q/TraceGC Ultra mass spectrometer; ion trap was used as the mass analyzer, the ionizing electron energy was 70 eV, the temperature of the ion source was 250°C, and the sample temperature was 50–450°C. IR spectra were measured on an FSM-1201 spectrometer in a Nujol (4000–400 cm^{-1} range) in KBr cells. The electronic absorption spectra of the complexes were recorded on a Perkin-Elmer Lambda 25 UV/Vis spectrometer (220–1100 nm range) at room temperature. The magnetic susceptibility (χ) of polycrystalline samples was determined using an MPMS*XL* SQUID magnetometer (Quantum Design) in the 2–300 K range with magnetic field of up to 5 kOe. The paramagnetic components of the magnetic susceptibility were found taking into account the diamagnetic contribution estimated from the Pascal constant. The effective magnetic moment was calculated by the formula $\mu_{eff} = [3k\chi T/(N_A\mu_B^2)]^{1/2}$, where N_A, μ_B, and k are the Avogadro number, Bohr magneton, and the Boltzmann constant, respectively. Mössbauer spectra were measured on an MS1104Em spectrometer. The Co^{57} in Rh matrix was used as the gamma-radiation source. On cooling, the samples were placed into a camera of a CCS-850 helium cryostat. The isomeric shifts δ were referred to α-Fe.

Synthesis of $(ImPh)_2FeCl$ (I). Weighed portions of $FeCl_3$ (0.13 g, 0.81 mmol) and (ImPh)H (0.5 g, 1.62 mmol) were dissolved in THF (15 mL). The addition of excess Et_3N (0.3 mL) to the resulting homogeneous reaction mixture was accompanied by instantaneous color change to red-brown and formation of a light-colored precipitate. The reaction mixture was kept for 15 min at room temperature, and the solvent was evaporated under reduced pressure. The dry residue was dissolved in toluene (15 mL), and the resulting solution was filtered through glass filter No. 4 to remove $[Et_3NH]Cl$. Complex **I** was crystallized from hexane (10 mL) by keeping the solution for 24 h at −18°C. The yield of the dark brown-green air-dried crystalline precipitate of **I** was 0.21 g (37%).

For $C_{42}H_{52}N_2O_2ClFe$

Anal. calcd., %	C, 71.23	H, 7.40	N, 3.96
Found, %	C, 71.62	H, 7.59	N, 3.88

EI-MS (*m/z*): 708 (100%), 709 (51%), 710 (42%), 711 (18%) $[M]^+$. UV/Vis (CH_2Cl_2), nm (ε, L mol^{-1} cm^{-1}): 230 (96279), 237 sh (92673), 262 (90912), 267 (87942), 302 sh (44163), 638 sh (1574). IR (ν, cm^{-1}): 1594 s, 1575 m, 1551 w, 1409 m, 1362 s, 1295 m, 1272 s, 1255 vs, 1224 s, 1203 m, 1182 w, 1160 m, 1130 w, 1028 w, 976 w, 957 m, 916 w, 886 w, 857 w, 833 s, 812 w, 772 w, 755 s, 691 s, 668 w, 644 w, 573 s, 559 w, 540 w, 495 w, 478 w.

Recrystallization of $(ImPh)_2FeCl$ (**I**) from *n*-hexane gave the crystals $\mathbf{I} \cdot 1.25C_6H_{14}$ suitable for X-ray diffraction.

Synthesis of $(ImPh)_2FeBr$ (II). The brown-green solution of **I** (0.25 g, 0.35 mol) in THF (10 mL) was added to KBr (0.42 g, 3.5 mmol) in methanol (10 mL). The resulting heterogeneous reaction mixture was stirred at room temperature for 3 days, with the color being changed to maroon-violet. The solvents were removed under reduced pressure, and the dry residue was dissolved in hexane (15 mL). The reaction mixture was separated from potassium halides by filtration. Complex **II** was isolated from the reaction mixture as a dark brown crystalline precipitate by keeping the preconcentrated filtrate at −18°C for 24 h. The yield is 0.08 g (31%).

For $C_{42}H_{52}N_2O_2BrFe$

Anal. calcd., %	C, 67.03	H, 6.96	N, 3.72
Found, %	C, 67.32	H, 7.14	N, 3.67

EI-MS (*m/z*): 752 (76), 753 (100), 754 (43%) $[M]^+$. UV/Vis (CH_2Cl_2) nm (ε, L mol^{-1} cm^{-1}): 274 (23786), 369 (11856), 653 (2105). IR (ν, cm^{-1}): 1594 s, 1575 s, 1551 m, 1445 vs, 1409 s, 1364 s, 1321 w, 1295 m, 1274 s, 1255 vs, 1222 s, 1205 m, 1186 w, 1160 m, 1127 w, 1025 w, 976 w, 959 m, 921 w, 914 w, 886 w, 864 w, 836 s, 812 w, 772 m, 755 s, 689 s, 668 w, 646 w, 620 w, 575 s, 540 m, 497 w, 483 w.

Synthesis of $(ImPh)_2FeI$ (III). The brown-green solution of **I** (0.25 g, 0.35 mol) in THF (10 mL) was

added to KI (0.59 g, 3.5 mmol) in methanol (10 mL). The reaction mixture was stirred at room temperature for 24 h; during this time, the KI precipitate dissolved and the solution color changed to maroon-red. The solvents were removed under reduced pressure, the dry residue was dissolved in toluene (15 mL), and the reaction mixture was separated from potassium halides by filtration. Toluene was removed from the filtrate under reduced pressure, the dry residue was dissolved in pentane (10 mL), and the solution was kept at −18°C for 24 h. Complex **III** was isolated from the reaction mixture as a dark brown crystalline solid. The yield was 0.12 g (42%).

For $C_{42}H_{52}N_2O_2FeI$

Anal. calcd., %	C, 63.09	H, 6.55	N, 3.50
Found, %	C, 63.37	H, 6.67	N, 3.43

EI-MS (*m/z*): 800 (100), 801 (57), 802 (47%) $[M]^+$. UV/Vis (CH_2Cl_2), nm (ε, L mol^{-1} cm^{-1}): 232 (27074), 270 (27626), 308 sh (22233), 367 (11734), 659 (2035). IR (ν, cm^{-1}): 1593 m, 1572 m, 1548 w, 1411 m, 1364 s, 1322 w, 1296 m, 1271 s, 1254 s, 1224 m, 1205 m, 1186 w, 1161 w, 1126 w, 1027 w, 976 w, 957 w, 915 w, 885 w, 864 w, 857 w, 836 s, 810 w, 773 w, 756 s, 691 m, 668 w, 647 w, 618 w, 574 m, 539 w, 497 w, 483 w.

Synthesis of $(ImPh)_2FeN_3$ (IV). The brown-green solution of **I** (0.25 g, 0.35 mol) in THF (20 mL) was added to the NaN_3 (0.23 g, 3.5 mmol). The reaction mixture was stirred at room temperature for 24 h; during stirring, the color of the mixture changed to maroon-red. The solvents were removed under reduced pressure, the dry residue was dissolved in toluene (15 mL), and the reaction mixture was separated from NaCl and NaN_3 precipitates by filtration. The solvent was removed from the filtrate under reduced pressure, the dry residue was dissolved in hexane (10 mL), and the solution was kept at −18°C for a week. Complex **IV** was isolated from the reaction mixture as a dark brown crystalline precipitate. The yield was 0.10 g (39%).

For $C_{42}H_{52}N_5O_2Fe$

Anal. calcd., %	C, 70.58	H, 7.33	N, 9.80
Found, %	C, 70.72	H, 7.49	N, 9.71

EI-MS (*m/z*): 713 (100%), 714 (78%), 715 (17%) $[M]^+$. UV/Vis (CH_2Cl_2), nm (ε, L mol^{-1} cm^{-1}): 231 (83736), 276 (31478), 357 (13819), 635 sh (1511). IR (ν, cm^{-1}): 2094 vs, 1594 s, 1575 m, 1551 w, 1409 s, 1362 s, 1298 m, 1272 s, 1255 vs, 1222 s, 1203 m, 1182 w, 1160 m, 1130 w, 1025 w, 980 w, 959 w, 914 w, 886 w, 859 w, 833 s, 812 w, 772 w, 755 s, 694 m, 687 m, 668 w, 644 w, 620 w, 594 w, 573 s, 540 w, 495 w, 478 w.

Synthesis of $(ImPh)_3Fe$ (V) was similar to the synthesis of complex **I**, but the reactant ratio was 1 : 3 (0.09 g of $FeCl_3$ (0.54 mmol) and 0.5 g of (ImPh)H (1.62 mmol)). Complex **V** was isolated from the reaction mixture as an orange-brown fine crystalline precipitate by keeping the preconcentrated solution in hexane at −18°C for 24 h. The yield was 0.11 g (21%).

For $C_{63}H_{78}N_3O_3Fe$

Anal. calcd., %	C, 77.12	H, 8.01	N, 4.28
Found, %	C, 77.41	H, 8.15	N, 4.19

EI-MS (*m/z*): 981 (100), 982 (71), 983 (13%) $[M]^+$. UV/Vis (CH_2Cl_2), nm (ε, L mol^{-1} cm^{-1}): 253 (40896), 306 (31934), 403 sh (14243), 485 sh (7632). IR (ν, cm^{-1}): 1596 s, 1575 m, 1549 w, 1497 m, 1411 s, 1359 s, 1284 vs, 1260 vs, 1236 s, 1222 s, 1203 s, 1182 m, 1158 s, 1130 w, 1025 w, 1002 w, 985 w, 968 m, 952 m, 931 w, 916 w, 883 m, 864 s, 833 vs, 810 m, 777 w, 750 vs, 691 s, 668 m, 641 w, 620 w, 604 w, 563 s, 554 s, 537 s, 495 m, 480 m.

X-ray diffraction. The diffraction data for the single crystal of $\mathbf{I}\cdot 1.25C_6H_{14}$ (0.50 × 0.31 × 0.13 mm) was collected on a Rigaku OD Xcalibur diffractometer (ω-scan mode, MoK_α-radiation, λ = 0.71073 Å, T = 298 K, 2θ = 54.2°). The CrysAlis^{Pro} [33] and SHELX [34] program packages were used to measure and integrate the experimental sets of intensities, to apply the absorption corrections, and to refine the structures. Compound **I** ($C_{42}H_{52}ClFeN_2O_2\cdot 1.25C_6H_{14}$) crystallizes in space group $P2_1/n$ (a = 16.0380(6), b = 13.6024(5), c = 24.0414(9) Å, β = 109.103(4)°, V = 4955.9(3) Å^3, Z = 4, $\rho_{calcd.}$ = 0.949 g/cm^3, μ = 0.386 mm^{-1}). Altogether 68869 reflections and 10896 unique reflections (R_{int} = 0.0427) were used to solve the structure and then to refine 550 parameters by the full-matrix least squares over F^2_{hkl} in the anisotropic approximation for nonhydrogen atoms. The hydrogen atoms in **I** were placed in geometrically calculated positions and refined isotropically with fixed thermal parameters $U(H)_{iso} = 1.2U(C)_{eq}$ ($U(H)_{iso} = 1.5U(C)_{eq}$ for methyl groups). The DFIX, ISOR, and RIGU restraints were used to restrict the geometric characteristics of the disordered *tert*-butyl groups and anisotropic displacement parameters in the structure refinement. The contribution of hexane solvation molecules to the structural model of **I** was included using the SQUEEZE procedure (Platon) [35]. After the final refinement, wR_2 = 0.1152 and $S(F^2)$ = 1.005 for all reflections (R_1 = 0.0400 for all reflections meeting the condition $I > 2\sigma(I)$). The residual electron density maximum and minimum were 0.26/−0.16 e/Å^3.

The structure of **I** was deposited with the Cambridge Crystallographic Data Centre (CCDC no. 1996527; ccdc.cam.ac.uk/structures).

RESULTS AND DISCUSSION

In view of the goal of this study, consisting in evaluating the role of radical ligands in the spin-crossover occurring in five-coordinate iron(III) derivatives, it was necessary to synthesize structurally similar metal compounds containing monoanionic diamagnetic O,N-chelating ligands to reproduce, as closely as possible, the coordination unit of the bis-*o*-iminobenzosemiquinolates $(ImSQ^R)_2Fe^{III}X$, where ImSQ is the singly reduced R-phenyl-substituted *o*-iminobenzoquinone and X is an inorganic anion (Scheme 1) [25–29].

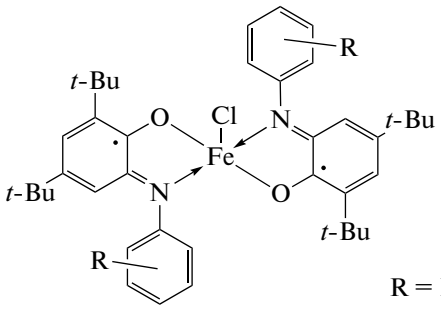

R = H, Me, OMe
X = Hal, N_3, NCO

$(ImSQ^R)_2FeX$

Scheme 1.

As the ligand system, we chose the Schiff base that is formed upon condensation of 4,6-di-*tert*-butyl-*o*-aminophenol with benzaldehyde. The subsequent exchange reaction between (ImPh)H and anhydrous $FeCl_3$ in 2 : 1 ratio carried out under anaerobic conditions in the presence of a base results in the formation of the target complex $(ImPh)_2FeCl$ (**I**) (Scheme 2).

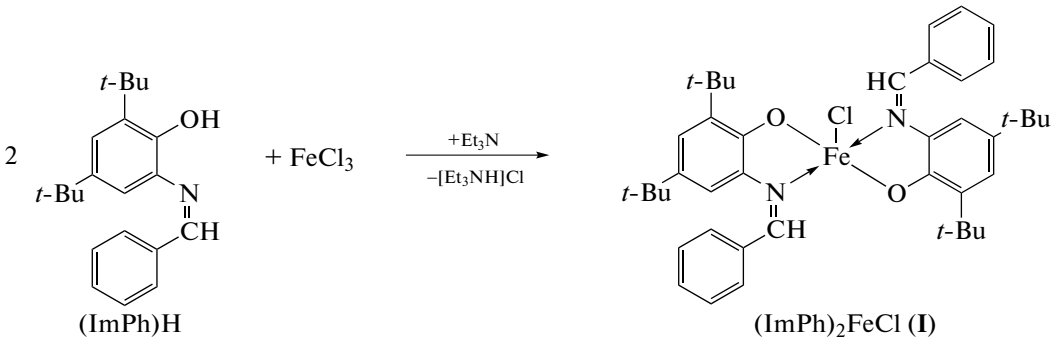

(ImPh)H

$(ImPh)_2FeCl$ (**I**)

Scheme 2.

The derivatives $(ImPh)_2FeX$ (X = Br (**II**), I (**III**), N_3 (**IV**)) were prepared by the reaction of **I** with a tenfold excess of KBr, KI, or NaN_3, respectively (Scheme 3).

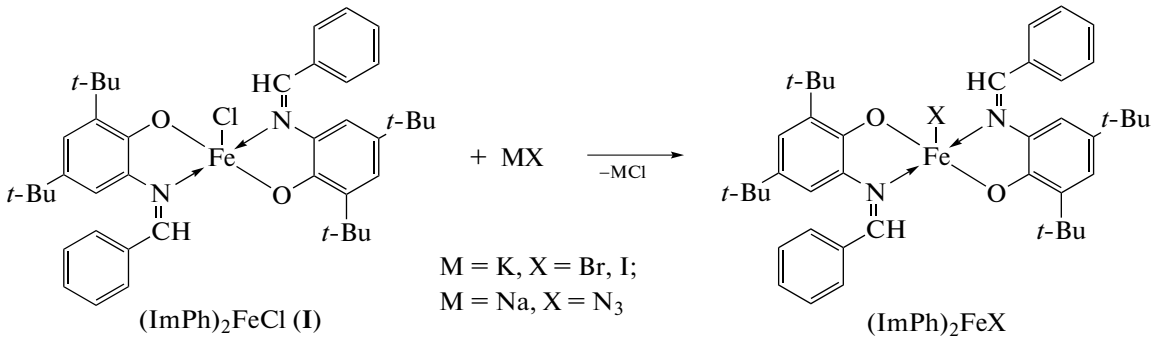

$(ImPh)_2FeCl$ (**I**)

M = K, X = Br, I;
M = Na, X = N_3

$(ImPh)_2FeX$
(X = Br (**II**), I (**III**), N_3 (**IV**))

Scheme 3.

Compounds **I**–**IV** were isolated from reaction mixtures as dark crystalline precipitates, stable in the anaerobic conditions. High solubility of **I**–**IV** in most organic solvents accounts for low preparative yields of the complexes (30–40%); in addition, presence of **I**–**IV** in solutions for a long time leads to symmetrization giving the fine crystalline tris-ligand orange complex $(ImPh)_3Fe$ (**V**). Complex **V** was also prepared via an alternative synthesis by the reaction of $FeCl_3$ with 3 equiv. of (ImPh)H (Scheme 4).

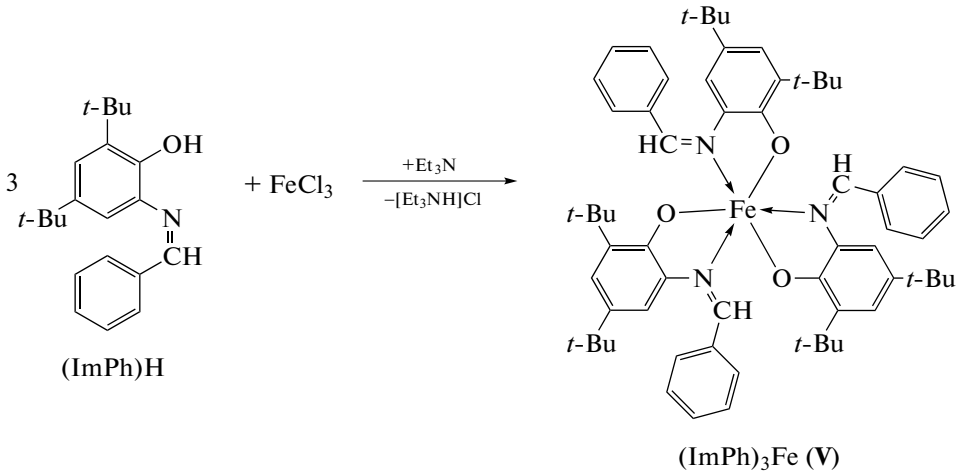

(ImPh)H

$(ImPh)_3Fe$ (**V**)

Scheme 4.

The IR spectra of **I**–**V** do not exhibit bands at 3100–3500 cm^{-1}, which are characteristic of the uncoordinated (ImPh)H ligand and correspond to ν(OH) stretching modes, which unambiguously attests to the formation of metal complexes. The bidentate coordination of the ImPh ligands to the metal is indicated by the shift of the C=N band (ν(C=N) is 1623 cm^{-1} in uncoordinated (ImPh)H, 1593–1594 cm^{-1} in **I**–**IV**, and 1596 cm^{-1} in **V**). In addition, the IR spectrum of **IV** exhibits an intense band at 2090 cm^{-1} for the $\nu(N_3)$ azide stretching mode. Apart from the molecular ion peak $[M]^+$ (see Experimental), the mass spectra of **I**–**IV** exhibit an intense peak corresponding to the $[(ImPh)_2Fe]^+$ fragment, that is $[M–X]^+$ (EI-MS (*m/z*): 672 (100), 673 (47), 674 (14%)). The presence of intense $[M–X]^+$ peak, along with $[M]^+$, attests to easy elimination of the substituent X under conditions of mass spectra recording. Previously, this type of behavior was observed for the mass spectra of similar five-coordinate trivalent metal bis-*o*-iminobenzosemiquinone derivatives $(ImSQ)_2MX$ (M = Al, Ga, Mn, Fe) [28, 29, 36–38]. The presence of a halogen atom in **I**–**III** and the absence of this atom in **V** was also established by the method proposed by Beilstein [39].

The electronic absorption spectra of complexes **I**–**V** were recorded in dichloromethane at 25°C in the 200–1000 nm range (Fig. 1). In the UV region and at the boundary with the visible region, the spectra of complexes **I**–**V** show highly intense absorption bands (Fig. 1b). The visible region contains a weak broadened band in the 500–900 nm range in the case of **I**–**IV**, while in the case of complex **V**, this band is absent (Fig. 1a). Note that related bis-*o*-iminobenzosemiquinolates such as $(ImSQ^R)_2Fe^{III}X$ [25–29], unlike **I**–**V**, exhibit a very intense absorption band in the near-IR region (700–850 nm), which is related to the radical anion nature of O,N-chelating ligands, giving rise to the ligand–ligand charge transfer (LLCT) band in the electronic absorption spectrum.

The X-ray diffraction study demonstrated that $(ImPh)_2FeCl$ (**I**) is a five-coordinate complex in which the metal cation is bound to two oxygen atoms and two nitrogen atoms of the ImPh ligands and to one chlorine atom (Fig. 2a). Selected bond lengths and angles of the complex are summarized in Table 1. The presence of two asymmetric chelate rings in $(ImPh)_2FeCl$ implies chirality of the metal center. According to X-ray diffraction data, the complex crystallizes in the centrosymmetric space group $P2_1/n$; the independent part of the unit cell contains one complex molecule in the general position. Thus, both isomers of **I** occur in the unit cell in 1 : 1 ratio (Fig. 2b). Note that the unit cell also contains hexane solvent molecules (five per four molecules of the complex). In other words, the complex $(ImPh)_2FeCl$ crystallizes as $\mathbf{I} \cdot 1.25C_6H_{14}$.

The coordination geometry of five-coordinate complexes and the degree of their distortion are often analyzed using the geometric parameter τ, which is zero for an ideal tetragonal pyramid and one for an ideal trigonal bipyramid [40]. For **I**, τ = 0.74 and the geometry of the FeN_2O_2Cl coordination polyhedron is

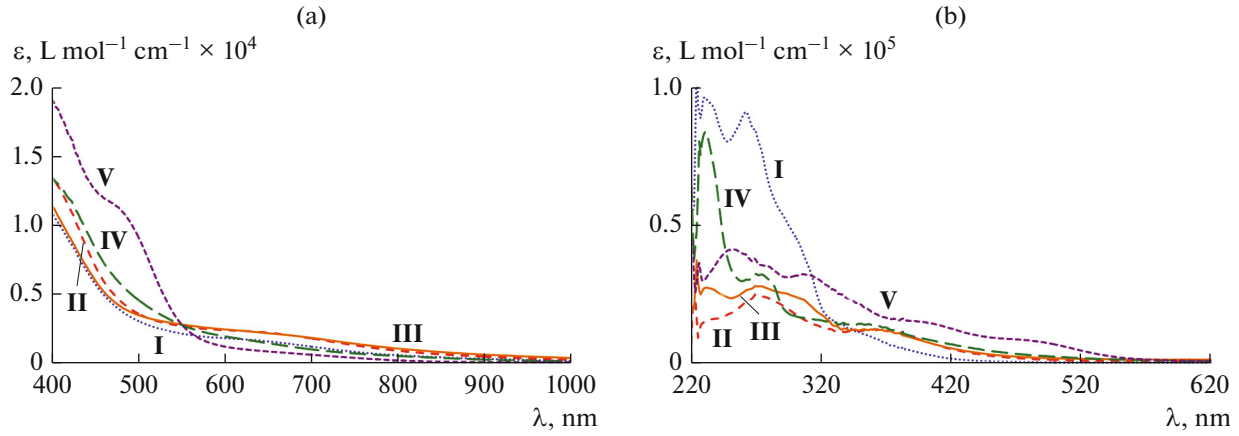

Fig. 1. UV/Vis spectra of complexes **I**–**V** measured in CH_2Cl_2 at 298 K.

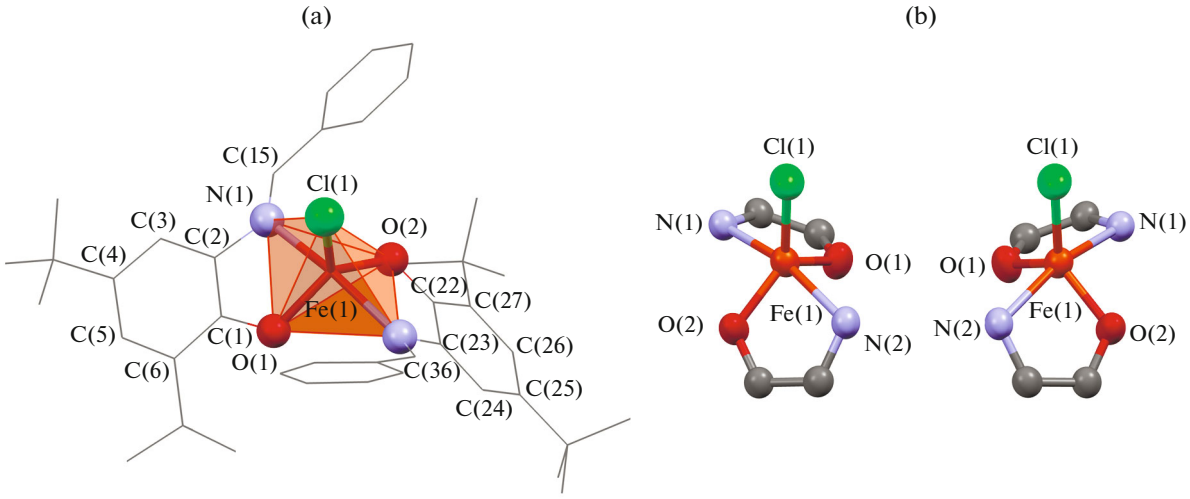

Fig. 2. (a) Molecular structure of complex **I** · 1.25C_6H_{14} (hydrogen atoms are omitted for clarity); (b) fragments of the structures of the two isomers of **I** · 1.25C_6H_{14} (thermal ellipsoids are drawn at the 50% probability level).

a distorted trigonal bipyramid, with the equatorial plane being formed by oxygen and chlorine atoms and the axial positions being occupied by nitrogen atoms. Notably, the τ value for bis-*o*-iminobenzosemiquinone derivatives $(ImSQ)_2FeX$ is in the 0–0.55 range [25–29]. Thus, transition from the ImSQ radical anion ligands to structurally similar diamagnetic ImPh ligands is accompanied by a change in the type of coordination geometry of the resulting complexes from a tetragonal pyramid to a trigonal bipyramid.

The C–O (1.343(2)–1.347(2) Å), C–N (1.426(2)–1.436(2) Å), and CH=N (1.287(2) Å) bond lengths are in the ranges typical of single C–O (1.32–1.37 Å), C–N (1.41–1.45 Å) and double CH=N (1.27–1.30 Å) bonds in the metal complexes with ligands of this type [41–44]. The C–C bond lengths in the C(1–6) and C(22–27) aromatic rings of ImPh (1.379(2)–1.411(2) Å, average 1.39 Å) are close to those in the benzene molecule (1.40 Å). The Fe–O bond lengths (1.868(2), 1.871(2) Å) are shorter than the sum of the covalent radii of the corresponding atoms ($r_{cov}(Fe^{III})$ = 1.36 Å, $r_{cov}(O)$ = 0.73 Å [45]), which is indicative of the covalent type of binding. Conversely, the Fe–N distances (2.187(2), 2.213(2) Å) considerably exceed the sum of the covalent radii of the corresponding atoms ($r_{cov}(Fe^{III})$ = 1.36 Å, $r_{cov}(N)$ = 0.74 Å [45]); thus, the Fe...N contacts in **I** can be classified as donor-acceptor bonds.

The magnetic susceptibility of crystalline samples **I**–**IV** was measured in the 2–300 K range. The temperature dependences of the effective magnetic moment $\mu_{eff}(T)$ for the series $(ImPh)_2FeX$ (X = Cl (**I**), Br (**II**), I (**III**), N_3 (**IV**)) are depicted in Fig. 3 and have similar shapes. For five-coordinate complexes **I**–**IV**, high-temperature μ_{eff} values (5.69, 5.88, 5.74, and 5.62 μ_B for **I**–**IV**, respectively) are close to the theoret-

Table 1. Selected bond lengths (Å) and angles (deg) in complex **I** · $1.25C_6H_{14}$

Bond	*d*, Å	Bond	*d*, Å
Fe(1)–O(1)	1.868(2)	C(1)–C(6)	1.411(2)
Fe(1)–O(2)	1.871(2)	C(2)–C(3)	1.396(2)
Fe(1)–N(1)	2.187(2)	C(3)–C(4)	1.379(2)
Fe(1)–N(2)	2.213(2)	C(4)–C(5)	1.398(3)
Fe(1)–Cl(1)	2.2294(6)	C(5)–C(6)	1.387(2)
O(1)–C(1)	1.347(2)	C(22)–C(27)	1.403(2)
O(2)–C(22)	1.343(2)	C(22)–C(23)	1.401(2)
N(1)–C(2)	1.436(2)	C(23)–C(24)	1.385(2)
N(2)–C(23)	1.426(2)	C(24)–C(25)	1.382(3)
N(1)–C(15)	1.287(2)	C(25)–C(26)	1.397(3)
N(2)–C(36)	1.287(2)	C(26)–C(27)	1.389(3)
Angle	ω, deg	Angle	ω, deg
O(1)Fe(1)O(2)	118.62(6)	N(1)Fe(1)N(2)	163.13(5)
O(1)Fe(1)N(1)	80.57(5)	O(1)Fe(1)Cl(1)	117.60(5)
O(2)Fe(1)N(1)	90.54(5)	O(2)Fe(1)Cl(1)	123.78(4)
O(1)Fe(1)N(2)	92.54(5)	N(1)Fe(1)Cl(1)	98.62(4)
O(2)Fe(1)N(2)	79.20(5)	N(2)Fe(1)Cl(1)	98.22(4)

ical spin-only value of 5.92 μ_B, calculated for a system containing high-spin iron(III) ion (d^5, HS, $S_{Fe} = 5/2$). As the temperature decreases down to 30 K, the μ_{eff} values change insignificantly, but on further cooling, it sharply decreases to reach 2.92, 2.89, 2.72, and 2.03 μ_B at a temperature of 2 K for **I**–**IV**, respectively. The decrease in μ_{eff} in the 30–2 K range is due to the intermolecular exchange interaction in crystalline **I**–**IV**.

Crystalline samples of **I**–**IV** were also characterized by Mössbauer spectroscopy. The Mössbauer spectra of complexes **II** and **V** are shown in Fig. 4, the spectral parameters for **I**–**IV** are summarized in Table 2. Decreasing temperature from 300 to 14 K does not induce significant spectral changes that would indicate a change in the spin state of the Fe^{3+} ion, which is in agreement with the data of magnetochemical measurements. The isomeric shifts (δ) for five-coordinate derivatives **I**–**IV** (0.30–0.52 mm s^{-1}) are close to those for five-coordinate bis-*o*-iminobenzosemiquinone derivatives $(ImSQ^{Me})_2FeX$ containing high-spin Fe^{3+} ion (HS, $S_{Fe} = 5/2$). Meanwhile, the quadrupole splitting values (ΔE_Q) for **I**–**IV** are 1.66–1.82 mm s^{-1}, which is somewhat higher than ΔE_Q for the mentioned $(ImSQ^{Me})_2FeX$ complexes (1.08–1.31 mm s^{-1}) [29]. The Mössbauer spectrum of the six-coordinate $(ImPh)_3Fe$ complex (**V**) (Fig. 4) differs from the spectra of five-coordinate $(ImPh)_2FeX$ complexes (**I**–**IV**) and has isomeric shift and quadrupole splitting parameters (0.29–0.41 and 1.96–1.98 mm s^{-1}, respectively) typical of octahedral low-spin iron(III) derivatives [2, 3]. This is in line with the magnetic susceptibility measurements for compound **V**: the effective magnetic moment at 14 K is 1.72 μ_B, which corresponds to one Fe^{3+} ion in the low-spin state (LS, $S_{Fe} = 1/2$).

Thus, in this study, we synthesized a series of five-coordinate iron(III) bis-*o*-iminophenolates $(ImPh)_2FeX$ (X = Cl (**I**), Br (**II**), I (**III**), N_3 (**IV**)),

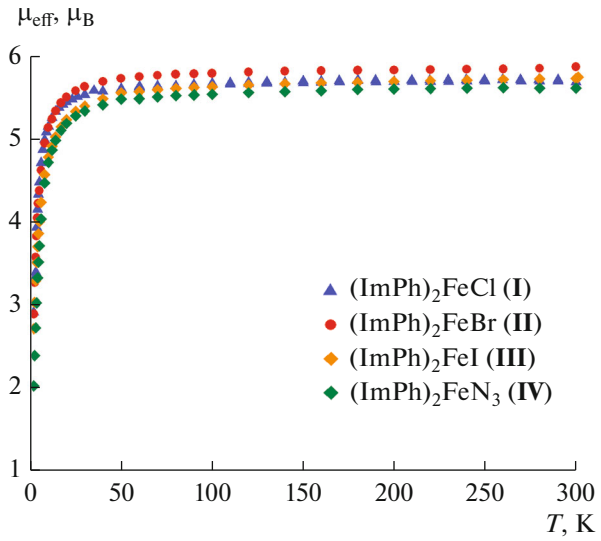

Fig. 3. Temperature dependences of the effective magnetic moment for $(ImPh)_2FeX$ (X = Cl (**I**), Br (**II**), I (**III**), N_3 (**IV**)).

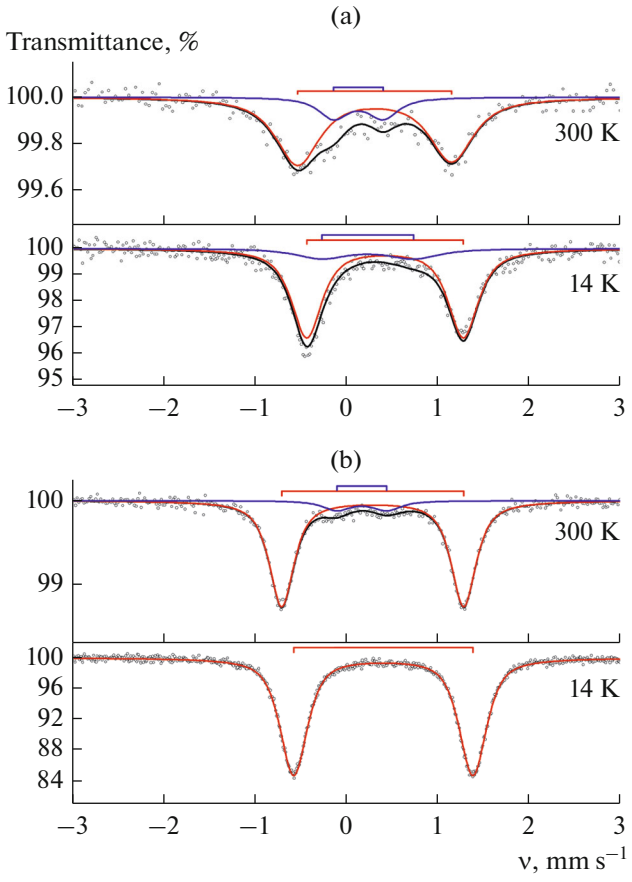

Fig. 4. Mössbauer spectra of complexes (a) **II** and (b) **V** measured at 300 and 14 K.

structural analogues of five-coordinate iron(III) bis-*o*-iminobenzosemiquinone derivatives. Although the (FeN_2O_2X) coordination core is the same for $(ImPh)_2FeX$ and $(ImSQ)_2FeX$ series, the structures of their coordination polyhedra are significantly different. Metal coordination of iminophenolate ligands results in two types of binding: covalent (Fe–O) and donor-acceptor (Fe–N) ones, which gives rise to a distorted trigonal-bipyramidal geometry of the resulting $(ImPh)_2FeX$ complexes. Conversely, the nature of the Fe–O and Fe–N bonds, resulting from much greater delocalization of the negative charge in the ImSQ radical anion ligand, promotes the formation of an ideal/distorted tetragonal-pyramidal geometry in $(ImSQ)_2FeX$. According to the set of available physicochemical data, the Fe^{3+} ion in iminophenolate complexes **I**–**IV** is in the high-spin state throughout the 2–300 K temperature range. This result implies that the radical anion nature of the O,N-chelating ImSQ ligands in the Fe^{3+} coordination sphere plays a key role for the spin-crossover in five-coordinate iron(III) derivatives with the FeN_2O_2X coordination core [25–30].

Table 2. Parameters of the Mössbauer spectra for complexes **I**–**V***

Complex	*T*, K	δ, mm s^{-1}	ΔE_Q, mm s^{-1}
I	300	0.36	1.72
	14	0.52	1.76
II	300	0.32	1.68
	14	0.43	1.72
III	300	0.30	1.68
	14	0.46	1.66
IV	300	0.33	1.70
	14	0.52	1.82
V	300	0.29	1.98
	14	0.41	1.96

* δ is isomeric shift, ΔE_Q is the quadrupole splitting.

ACKNOWLEDGMENTS

The studies were carried out using research equipment of the Center for Collective Use "Analytical Center of the Razuvaev Institute of Organometallic Chemistry, Russian Academy of Sciences" at the Razuvaev Institute of Organometallic Chemistry, Russian Academy of Sciences and supported by the Federal Research Program "Research and Development in the Priority Areas of the Science and Technology Sector of Russia for 2014–2020" (unique identifier of the project: RFMEFI62120X0040).

FUNDING

The study was supported by the Russian Science Foundation (project no. 18-73-00268).

CONFLICT OF INTEREST

The authors declare that they have no conflict of interest.

REFERENCES

1. van Koningsbruggen, P.J., Maeda, Y., and Oshio, H., *Top. Curr. Chem.*, 2004, vol. 233, p. 259.
2. Nihei, M., Shiga, T., Maeda, Y., and Oshio, H., *Coord. Chem. Rev.*, 2007, vol. 251, p. 2606.
3. Harding, D.J., Harding, P., and Phonsri, W., *Coord. Chem. Rev.*, 2016, vol. 313, p. 38.
4. Ksenofontov, V., Gaspar, A.B., and Gutlich, P., *Top. Curr. Chem.*, 2004, vol. 235, p. 23.
5. Hauser, A., *Top. Curr. Chem.*, 2004, vol. 234, p. 155.
6. Létard, J.-F., *J. Mater. Chem.*, 2006, vol. 16, p. 2550.
7. Cannizzo, A., Milne, C.J., Consani, C., et al., *Coord. Chem. Rev.*, 2010, vol. 254, p. 2677.
8. Bousseksou, A., Varret, F., Goiran, M., et al., *Top. Curr. Chem.*, 2004, vol. 235, p. 65.
9. Halcrow, M.A., *Spin-Crossover Materials, Properties and Applications*, New York: Wiley, 2013.

10. Starikova, A., Starikov, A.G., and Minkin, V.I., *Russ. Chem. Bull.*, 2016, vol. 65, p. 1464.
11. Starikova, A.A., Starikov, A.G., and Minkin, V.I., *Russ. J. Coord. Chem.*, 2017, vol. 43, p. 718. https://doi.org/10.1134/S1070328417110094
12. Starikov, A.G., Chegerev, M.G., Starikova, A.A., and Minkin, V.I., *Russ. J. Coord. Chem.*, 2019, vol. 45, p. 675. https://doi.org/10.1134/S1070328419090082
13. Starikov, A.G., Starikova, A.A., Chegerev, M.G., and Minkin, V.I., *Russ. Chem. Bull.*, 2019, vol. 68, p. 725.
14. Starikova, A.A., Chegerev, M.G., Starikov, A.G., and Minkin, V.I., *J. Comput. Chem.*, 2019, vol. 40, p. 2284.
15. Starikova, A.A., Metelitsa, E.A., and Starikov, A.G., *J. Struct. Chem.*, 2019, vol. 60, p. 1219.
16. Earnshaw, A., King, E.A., and Larkworthy, L.F., *Chem. Commun*. (London), 1965, p. p. 180.
17. Earnshaw, A., King, E.A., and Larkworthy, L.F., J. Chem. Soc. A, 1969, p. 2459.
18. Haller, K.J., Johnson, P.L., Feltham, R.D., et al., *Inorg. Chim. Acta*, 1979, vol. 33, p. 119.
19. Fitzsimmons, B.W., Larkworthy, L.F., and Rogers, K.A., *Inorg. Chim. Acta*, 1980, vol. 44, p. L53.
20. Wells, F.V., McCann, S.W., Wickman, H.H., et al., *Inorg. Chem.*, 1982, vol. 21, p. 2306.
21. Koenig, E., Ritter, G., Waigel, J., et al., *Inorg. Chem.*, 1987, vol. 26, p. 1563.
22. Weber, B., Gorls, H., Rudolph, M., and Jäger, E.-G., *Inorg. Chim. Acta*, 2002, vol. 337, p. 247.
23. Nakamura, M., *Coord. Chem. Rev.*, 2006, vol. 250, p. 2271.
24. Ohgo, Y., Chiba, Y., Hashizume, D., et al., *Chem. Commun.*, 2006, p. 1935.
25. Chun, H., Weyhermüller, T., Bill, E., and Wieghardt, K., *Angew. Chem., Int. Ed. Engl.*, 2001, vol. 40, p. 2489.
26. Chun, H., Bill, E., Weyhermüller, T., and Wieghardt, K., *Inorg. Chem.*, 2003, vol. 42, p. 5612.
27. Abakumov, G.A., Cherkasov, V.K., Bubnov, M.P., et al., *Russ. Chem. Bull. Int. Ed.*, 2006, vol. 55, p. 44.
28. Piskunov, A.V., Pashanova, K.I., Ershova, I.V., et al., *J. Mol. Struct.*, 2018, vol. 1165, p. 51.
29. Ershova, I.V., Bogomyakov, A.S., Kubrin, S.P., et al., *Inorg. Chim. Acta*, 2020, vol. 503, p. 119402.
30. Credendino, L. and Sproules, S., *Asian J. Org. Chem.*, 2019, vol. 9, p. 421.
31. Perrin, D.D., Armarego, W.L.F., and Perrin, D.R., *Purification of Laboratory Chemicals*, Oxford: Pergamon, 1980.
32. Yasuhiko, S., Norio, K., and Terunori, F., *Chem. Lett.*, 2002, vol. 31, p. 358.
33. *Rigaku Oxford Diffraction. CrysAlis^{Pro} Software System. Version 1.171.38.46*, Wroclaw: Rigaku Corporation, 2015.
34. Sheldrick, G.M., *Acta Crystallogr., Sect. C: Struct. Chem.,* 2015, vol. 71, p. 3.
35. Spek, A.L., *Acta Crystallogr., Sect. C: Struct. Chem.,* 2015, vol. 71, p. 9.
36. Piskunov, A.V., Ershova, I.V., Bogomyakov, A.S., et al., *Inorg. Chem.*, 2015, vol. 54, p. 6090.
37. Piskunov, A.V., Ershova, I.V., Bogomyakov, A.S., and Fukin, G.K., *Inorg. Chem. Commun.*, 2016, vol. 66, p. 94.
38. Ershova, I.V., Bogomyakov, A.S., Fukin, G.K., and Piskunov, A.V., *Eur. J. Inorg. Chem.*, 2019, vol. 2019, p. 938.
39. Beilstein, F., *Ber. Dtsch. Chem. Ges.*, 1872, vol. 5, p. 620.
40. Addison, A.W., Rao, T.N., Reedijk, J., et al., *Dalton Trans.*, 1984, p. 1349.
41. Mukherjee, S., Weyhermüller, T., Bothe, E., and Chaudhuri, P., *Eur. J. Inorg. Chem.*, 2003, vol. 2003, p. 1956.
42. Suzuki, Y., Tanaka, H., Oshiki, T., et al., *Chem. Asian J.*, 2006, vol. 1, p. 878.
43. Zhang, L., Luo, X., Gao, W., et al., *Organometallics*, 2013, vol. 32, p. 6277.
44. Safaei, E., Alaji, Z., Panahi, F., et al., *New J. Chem.*, 2018, vol. 42, p. 7230.
45. Batsanov, S.S. *Russ. J. Inorg. Chem.* 1991, vol. 36, p. 1694.

Translated by Z. Svitanko